MONITORING OF POSSIBLE IONOSPHERIC DISTURBANCES CAUSED BY VAN EARTHQUAKE (Mw 7.2) USING GNSS MEASUREMENTS

Selcuk PEKER[1], Samed INYURT [2] and Cetin MEKIK[2]

1 General Command of Mapping, Ankara, Turkey (selcuk-peker@hotmail.com)
2Bulent Ecevit University, Geomatics Engineering Department, Zonguldak (samed_inyurt@hotmail.com, cmekİk@hotmail.com)

ABSTRACT

Several scientists from different disciplines have studied earthquakes for many years. As a result of these studies, it has been proposed that some changes take place in the ionosphere layer before, during or after earthquakes, and the ionosphere should be monitored in earthquake prediction studies. This study investigates the changes in the ionosphere created by the earthquake with magnitude of Mw=7.2 in the northwest of the Lake Erçek which is located to the north of the province of Van in Turkey on 23 October 2011 and at 1.41 pm local time (-3 UT) with the epicenter of 38.758° N, 43.360° E using the TEC values obtained by the Global Ionosphere Models (GIM) created by IONOLAB-TEC and CODE. In order to see whether the ionospheric changes obtained by the study in question were caused by the earthquake or not, the ionospheric conditions were studied by utilizing indices providing information on solar and geomagnetic activities (F10.7 cm, Kp, Dst).

As a result of the statistical test on the TEC values obtained from the both models, positive and negative anomalies were obtained for the times before, on the day of and after the earthquake, and the reasons for these anomalies are discussed in detail in the last section of the study. As the ionospheric conditions in the analyzed days were highly vibrant, it was thought that the anomalies were caused by geomagnetic effects, solar activity and the earthquake. The authors believe that interdisciplinary studies are needed to distinguish the earthquake-related part of the anomalies in question.

Keywords: TEC, Van Earthquake, Ionosphere

1. INTRODUCTION

The ionosphere is the part of the atmosphere at the altitudes of 60 km to 1.100 km where there are ions and free electrons in considerable amounts that can reflect electromagnetic waves (URL-1). It completely covers the thermosphere, one of the main layers of the atmosphere, but also includes some of the mesosphere and the exosphere.

The atmospheric gas molecules in the layer in question are charged with electricity influenced by the UV radiation from sunlight and disintegrating into ions and electrons, hence leading to ionization. As a result of this ionization, especially the fields of information and communication technologies, intensely using audio, data and signal interactions, are affected by the ionosphere (Anderson and Fuller-Rowell, 1999)

When a radio wave reaches the ionosphere, the electric component of the electromagnetic wave forces the electrons in the ionosphere to vibrate in the same frequency as the radio wave. The vibration energy leads to reorganization of the electrons or the electrons' replication of the original radio frequency. If the plasma frequency is lower than the radio frequency and the quantity of electrons is sufficient, complete reflection occurs. If the frequency of the radio wave is higher than the plasma frequency of the ionosphere, electrons cannot provide feedback fast enough, and thus the signal is not reflected.

The most important parameter that defines the ionosphere in space and time is the quantity of electrons. This quantity varies under the influence of the day-night cycle, seasons, geographical location and magnetic storms in the sun. As it is not possible to measure the quantity of electrons in the ionosphere directly, indirect measurement and calculation methods have been developed (Li and Parrot, 2018). Total Electron Content (TEC), which is defined as the quantity of free electrons along a cylinder with a cross section of 1 m^2, is a suitable parameter to monitor the changes in the ionosphere in space and time. All signals that contain audio and data that pass through or get reflected from the ionosphere, which is highly irregular and difficult to model, are affected by the structure of this layer.

Calculating Total Electron Content (TEC) is a method used directly to investigate the structure of the ionosphere. TEC is represented by the unit of TECU, and one TECU equals to $10^{16}\ el/m^2$ (Schaer, 1999). TEC is expressed in two ways: STEC (Slant Total Electron Content); the free electron content calculated along the slanted line between the receiver and the satellite, and VTEC (Vertical Total Electron Content); the free electron content calculated along the zenith of the receiver (Langley, 2002).

TEC varies based on positional and temporal variables such as the latitude of the place, seasons, solar activity, geomagnetic storms and earthquakes. Ionospheric altitude also differs based on geography.

TEC, which is defined as the number of free electrons on the one square meter area on the line followed by a radio wave, is one of the important parameters for examining the structure of the ionosphere and the upper atmosphere. With TEC values, it is possible to examine the short and long-term changes in the ionosphere, ionospheric irregularities and disruptive factors together (Erol and Arıkan 2005; Başpınar 2012).

The changes in the ionosphere created by earthquakes were first studied in early 1960s. In order to detect any prior sign before earthquakes, experts examined the critical frequency, the maximum electron density in the F2 layer and total electron content (Yildirim et al., 2016). Some studies have shown that ionospheric anomalies may be detected in a short time before earthquakes using satellites (Pulinets 1998; Rozhnoi et al., 2015).

Ionospheric changes are being studies in more than twenty countries today as precursors of earthquakes. Definition of ionospheric anomalies and feasibility studies of seismo-ionospheric precursors are still ongoing (Liu et al., 2010; He et al., 2012; Pulinets and Davidenko, 2014; Yildirim et al., 2016; He and Heki, 2017; Kelley et al., 2017; Akhoonzadeh et al., 2018).

2. METHODOLOGY

2.1 IONOLAB-TEC Method:

The IONOLAB-TEC method developed by the department of Electrical and Electronics Engineering of Hacettepe University is a JAVA application that uses the Regularized TEC (D-TEI) algorithm (Arikan et al. 2004).

In this application, they developed a method that estimates VTEC values by using all GPS signals measured at a period of time in a day. While the measurements taken from the satellites with elevations of 60^o or higher are used, the measurements from the satellites with elevations of $10^o\ to\ 60^o$ are weighted by a Gauss function. The data from satellites with elevations of lower than 10^o are not included in calculations to reduce multipath effects (Equations 1).

$$\left.\begin{cases} \omega_m(n) & \begin{array}{ll} 1, & 60^o \leq \epsilon_m\ (n) \leq 90^o \\ \exp(-(60-\epsilon_m\ (n))^2/2\sigma^2)\ , & 10^o \leq \epsilon_m\ (n) < 60^o \\ 0, & \epsilon_m\ (n) < 10^o \end{array} \end{cases}\right\} \quad (1)$$

In the next step, the VTEC data obtained from satellites are combined by the least squares method. For this, a cost function that will minimize the square of the error between the VTEC data that will be obtained as a result of estimation, and the VTEC data calculated from the satellites is defined as below.

$$J_{\mu.k_c}(x) = \sum_{m=1}^{M}(x-x_m)^2 W_m(x-x_m) + \mu x^T H(k_c) \quad (2)$$

$W_m = diag(w_m)$,

$\mathrm{H}(k_c)$ = Filter that allows components of frequencies up to k_c to pass,

μ = Regularization coefficient.

To find the x estimates that minimize the error, if the derivative of the statement in Equation (2) is taken and equated to 0;

$$(\Delta_x J_{\mu,k_c}(x)) = 0 \quad (3)$$

The minimization process for the cost function turns into the solution of a linear system like:

$$A(\mu, k_c)x = b \quad (4)$$

In the equation above:

$$A(\mu, k_c) = \sum_{m=1}^{M} W_m + \mu H(k_c) \quad (5)$$

$$b = \sum_{m=1}^{M} W_m x_m \quad (6)$$

Therefore, the VTEC estimates $\tilde{\mathbf{x}}$ are found as,

$$\tilde{X}(\mu, k_c) = A^{-1}(\mu, k_c)b \quad (7)$$

The high-pass penalty filter used for TEC estimates may be organized as the $\mathbf{H}(k_c)$ Toeplitz matrix:

$$\mathbf{H}(k_c) = \begin{bmatrix} h_0(k_c) & h_1(k_c)\,\Lambda & h_{N-1}(k_c) \\ h_{N-1}(k_c) & h_0(k_c)\,\Lambda & h_{N-2}(k_c) \\ \mathrm{M} & \mathrm{M} & \mathrm{M} \\ h_1(k_c) & h_2(k_c)\,\Lambda & h_0(k_c) \end{bmatrix} \quad (8)$$

$$h_n(k_c) = \frac{1}{N}\sum_{k=0}^{N-1} H_k(\omega_c)\exp(j\frac{2\pi}{N}kn) \quad (9)$$

$\omega_c = 2\pi k_c/N$. The filter function $\mathbf{H}_k(\omega_c)$ may be chosen as in Equation (11).

$$H_k(\omega_c) = \begin{cases} 1, & \text{if } \pi - \omega_c \le \dfrac{2\pi}{N} k \le \pi + \omega_c \\ 0, & \text{diger} \end{cases} \tag{10}$$

$$h_n(k_c) = \begin{cases} 1 - \dfrac{1}{N}(2k_c + 1), & n = 0 \\ -sin\left(\dfrac{\pi n}{N}(2k_c + 1)\right) \Big/ \left(N\, sin(\dfrac{\pi n}{N})\right), & n \neq 0 \end{cases} \tag{11}$$

The error function between the VTEC values calculated from satellites $\mathbf{x}_m$ and the VTEC estimates $\tilde{\mathbf{x}}$ is given in Equation (12). The operation ||.|| describes the norm statement of the difference vector weighted between the VTEC estimates and calculations.

$$e(\mu, k_c) = \sum_{\mathbf{m}=1}^{M} \left\| \mathrm{W}_{\mathbf{m}} (\tilde{\mathbf{x}} - \mathbf{x}_{\mathbf{m}}) \right\|^2 \tag{12}$$

In order to regularize the estimate values even more, floating median filter may be used. The length of the median filter is another parameter to be determined. With the estimated VTEC values, post-estimation median filter was applied, and the error function between the VTEC values is given in Equation (13).

$$e_f(N_f) = \left\| \tilde{\mathbf{x}} - \tilde{\mathbf{x}}_{\mathbf{N_f}} \right\|^2 \tag{13}$$

In Equation (13), $\tilde{\mathbf{x}}_{N_f}$ shows the $\tilde{\mathbf{x}}$ estimates processed with a median filter with the length of N_f. For the method to work accurately, suitable μ, k_c and N_f parameters must be determined. The details provided up to now cover the regularization method for a period of 24 hours.

When there is an estimation of TEC for a limited period of time, the cost function is redefined as in Equation (14).

$$J_{\mu,k_c}(x) = \sum_{m=1}^{M} (x - x_m)^T \, W_m (x - x_m) + \mu (x - at)^T H(k_c)(x - at) \tag{14}$$

In the equation, a is the slope of the line and $\mathbf{t}$ is the time vector for the period of time. In order to find $\mathbf{x}$ estimates that minimize the cost function, the derivative of this function is taken, and the result is equated to zero. In this case, minimization of the cost function is turned into the solution of a system of equations as in Equation (15).

$$\mathrm{A}(\boldsymbol{\mu},\mathbf{k_c})\begin{bmatrix}\mathbf{x}\\ \mathrm{a}\end{bmatrix} = \mathrm{b} \tag{15}$$

The matrix **A** in Equation (16) and the vector **b** in Equation (17) are calculated as,

$$\mathbf{A}(\mu,k_c) = \begin{bmatrix} \sum_{m=1}^{M}\mathbf{W}_m + \mu\mathbf{H}(k_c) & -\mu\mathbf{H}(k_c) \\ \mathbf{t}^T\mathbf{H}(k_c) & -\mathbf{t}^T\mathbf{H}(k_c)\mathbf{t} \end{bmatrix} \tag{16}$$

$$\mathbf{b} = \begin{bmatrix} \sum_{m=1}^{M} \mathbf{W}_m \mathrm{x}_m \\ 0 \end{bmatrix} \tag{17}$$

Using the equations above, the $\tilde{\mathbf{x}}$ values showing the **x** estimates are calculated as in Equation (18).

$$\begin{bmatrix}\tilde{\mathrm{x}}(\boldsymbol{\mu},\boldsymbol{k}_c)\\ \boldsymbol{a}\end{bmatrix} = \boldsymbol{A}^{-1}(\boldsymbol{\mu},\boldsymbol{k}_c)\boldsymbol{b} \tag{18}$$

As a result, the proposed regularization method may be applied for both day-long and limited periods of time (Arıkan et al. 2004).

2.2 Global Ionosphere Model (GIM):

Global Ionospheric Maps are published in the IONEX (IONosphere map EXchange) format in a way that covers the entire world. The institutions that produce these maps in the world include CODE (Center for Orbit Determination in Europe, Switzerland), DLR (Fernerkundungstation Neustrelitz, Germany), ESOC (European Space Operations Centre, Germany), JPL (Jet Propulsion Laboratory, California), NOAA (National Oceanic and Atmospheric Administration, United States), NRCan (National Resources, Canada), ROB (Royal Observatory of Belgium, Belgium), UNB (University of New Brunswick, Canada), UPC (Polytechnic University of Catalonia, Spain), WUT (Warsaw University of Technology, Poland) (Aysezen, 2008). In this study we used the GIM-TEC values produced by CODE in the IONEX format. In the dates they were analyzed, the temporal resolution of the TEC values was 2 hours, while their positional resolution was 2.5º by latitude and 5º by longitude. In order to calculate TEC values for a point whose latitude and longitude is known on the GIM-TEC maps created by CODE using more than 300 GNSS receivers around the world, the 4 TEC values that cover the point and the two-variable interpolation formula are given below (Schaer et al. 1998).

$$E_{int}(\lambda_0 + p\Delta\boldsymbol{\lambda}, \beta_0 + q\Delta\beta) = (1-p)(1-q)E_{0.0} + p(1-q)E_{1.0} + q(1-p)E_{0.1} + pqE_{1.1} \quad (19)$$

p and q: $0 \leq p, q < 1$.

$\Delta\lambda$ and $\Delta\beta$: Longitude and Latitude differences grid widths,

λ_0 *and* β_0: Initial longitude and latitude values,

$E_{0.0}, E_{1.0}, E_{0.1}$ *ve* $E_{1.1}$: TEC values known in neighboring points,

E_{int}: TEC value to be found.

3. ANALYSIS TO DETERMINE EARTHQUAKE-RELATED TEC CHANGES

In order to investigate earthquake-related TEC changes, the TEC values for the stations close to the epicenters, HAKK, MALZ, OZAL and TVAN were procured using the IONOLAB-TEC and GIM-TEC models. The correlation coefficient was obtained for the TEC values from both models between the dates 13.10.2011 and 02.11.2011 for the stations above.

Figure 1. Analyzed Stations

Figure 3 shows the stations analyzed (represented by red triangles) and the epicenter of the earthquake represented by blue star. For each station, the TEC values with the temporal resolution of two hours obtained from both the IONOLAB-TEC and GIM-TEC models and the correlation coefficient showing whether there is a linear relationship between two values were calculated as below;

$$r = \frac{\sum(xy) - (\sum x)(\sum y)/n}{\sqrt{(\sum x^2 - (\sum x)^2/n)(\sum y^2 - (\sum y)^2/n)}} \tag{20}$$

In order to determine the outlier values among the TEC values with a two-hour temporal resolution from both models, the TEC values obtained from both models between the dates 01.10.2011 and 10.10.2011, which were considered calm in terms of geomagnetic and solar activity, were used to determine the upper boundary (UB) and the lower boundary (LB). By utilizing the TEC values from both models, the UB and LB values were calculated using the formulae x+3σ and x-3σ. Here, x is the mean TEC value for the relevant epoch and σ is the standard deviation. If the TEC value in any epoch is higher than the upper boundary, it is a positive anomaly. Similarly if it is lower than the lower boundary, it is a negative anomaly. In order to investigate whether the anomalies before, on the day of and after the earthquake were caused by the earthquake or not, we also examined the (Kp*10), Dst and F10.7 cm indices, which provided information on the geomagnetic and solar activity for the days in which anomalies were detected.

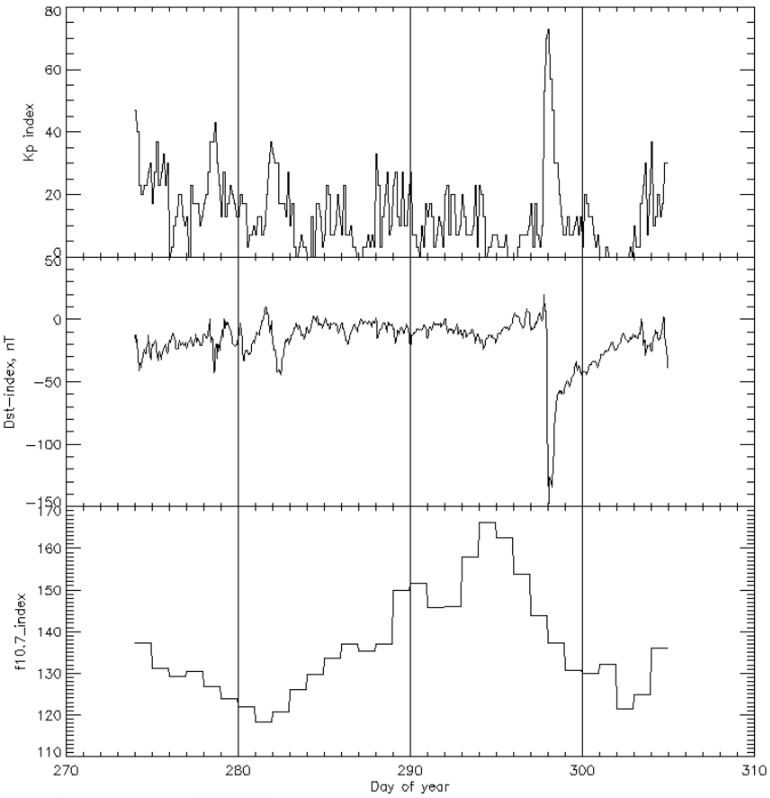

Figure 2. The Chart for October 2011 (Kp*10), Dst and F10.7 cm Indices (URL-2)

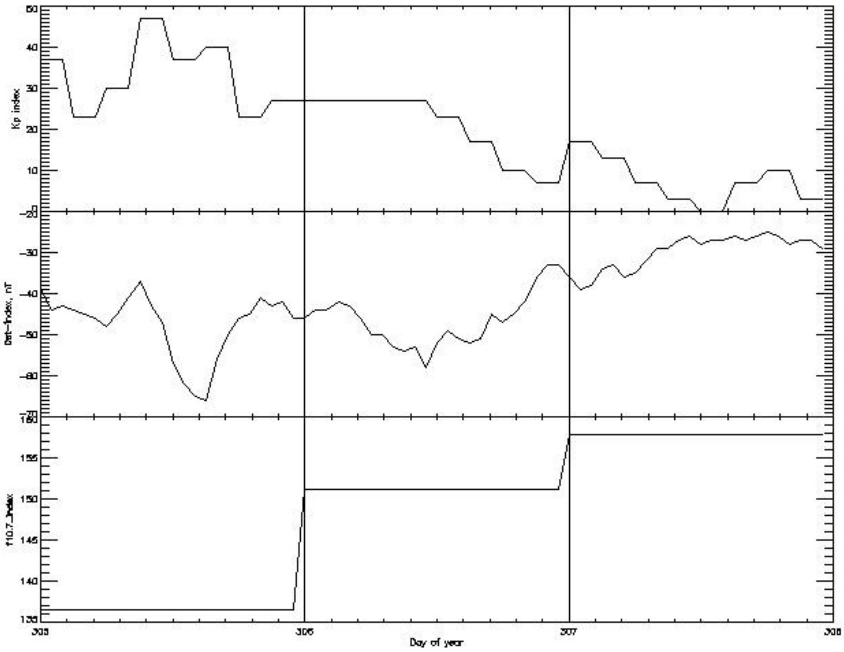

Figure 3. The Chart for the Dates 01-03.11.2011 in (Kp*10), Dst and F10.7 cm Indices (URL-2)

Figures 4 and 5 show the (Kp*10), Dst and F10.7 cm indices that provide information on geomagnetic and solar activity in October and on the first three days of November. Below are the TEC values for the HAKK station for the dates 13.10.2011-02.11.2011 obtained using the GIM-TEC and IONOLAB-TEC methods (Figures 6 and 7).

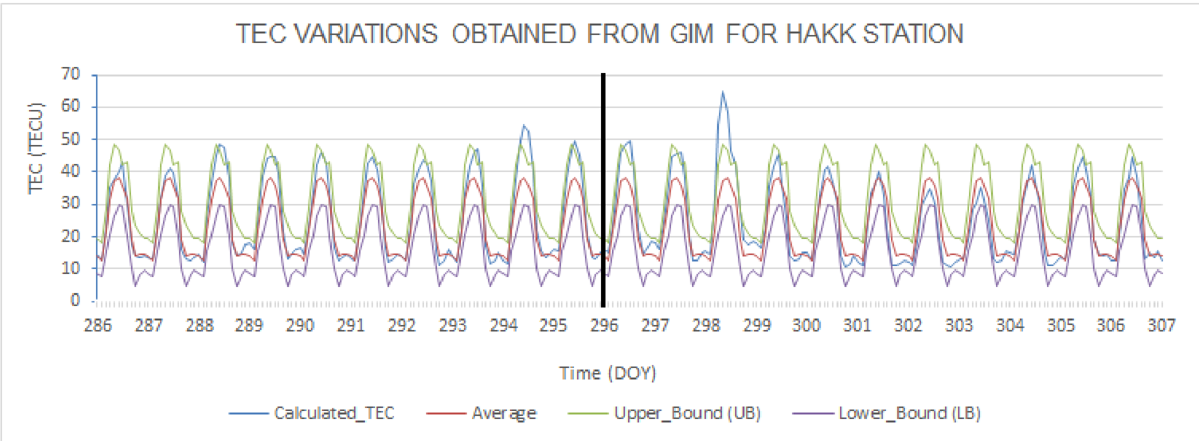

Figure 4. GIM-TEC Values for the HAKK Station

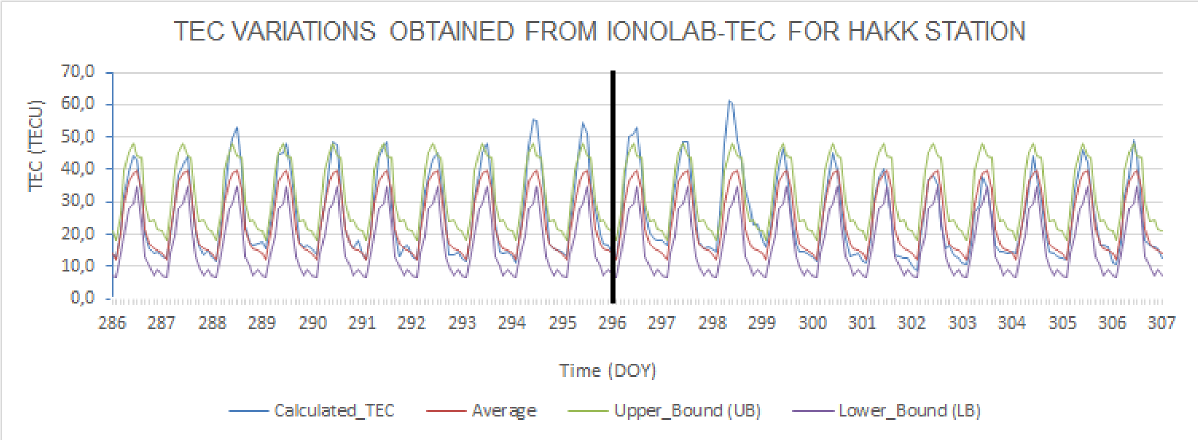

Figure 5. IONOLAB-TEC Values for the HAKK Station

The correlation coefficient ***r*** between the TEC values calculated by both methods for the HAKK station was 0.978469 indicating a strong positive relationship. The anomaly tables for this station are provided below (Tables 1 and 2).

GIM-TEC Anomaly Table for HAKK Station									
Number	**DOY**	**Hour**	**TEC Difference (TECU)**	**Type of Anomaly**	**Number**	**DOY**	**Hour**	**TEC Difference (TECU)**	**Type of Anomaly**
1	286	12	1.0	Positive	7	294	12	10.5	Positive
2	288	12	5.7	Positive	8	295	12	7.3	Positive
3	289	12	2.5	Positive	9	296	12	7.5	Positive
4	290	12	0.5	Positive	10	297	12	4.1	Positive
5	292	12	0.8	Positive	11	298	8	16.5	Positive
6	293	12	5.2	Positive					

Table 1. HAKK Station Global Ionosphere Model Anomaly Table

IONOLAB-TEC Anomaly Table for HAKK Station									
Number	**DOY**	**Hour**	**TEC Difference (TECU)**	**Type of Anomaly**	**Number**	**DOY**	**Hour**	**TEC Difference (TECU)**	**Type of Anomaly**
1	287	12	0.4	Positive	9	295	12	7.2	Positive
2	288	12	9.2	Positive	10	296	12	8.8	Positive
3	289	12	4.3	Positive	11	297	12	4.6	Positive
4	290	12	3.8	Positive	12	298	8	16.5	Positive
5	291	12	4.5	Positive	13	301	12	0.3	Negative
6	292	12	1.4	Positive	14	302	14	0.9	Negative
7	293	12	4.2	Positive	15	303	12	0.7	Negative
8	294	12	10.9	Positive	16	306	10	0.9	Positive

Table 2. HAKK Station IONOLAB-TEC Anomaly Table

Below are the TEC values for the MALZ station obtained using the GIM-TEC and IONOLAB-TEC methods (Figures 8 and 9).

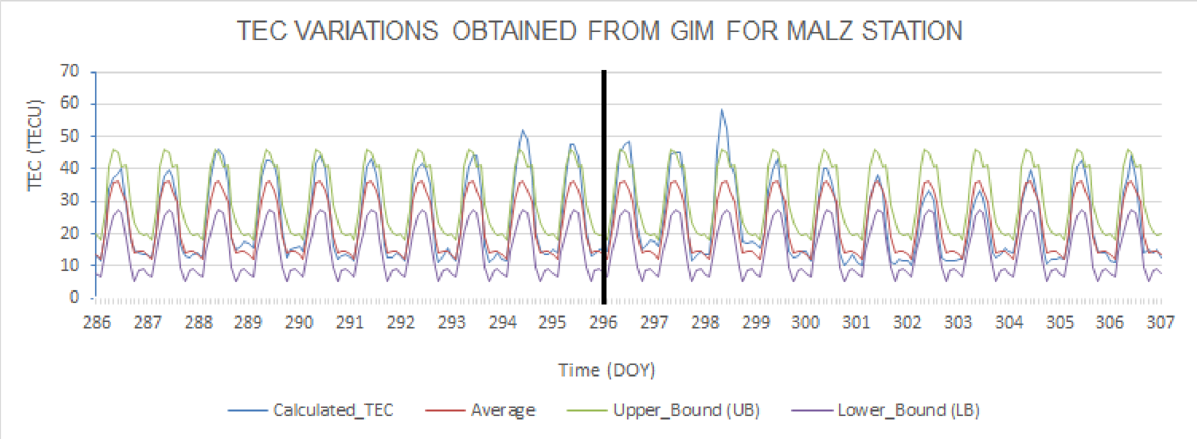

Figure 6. GIM-TEC Values for the MALZ Station

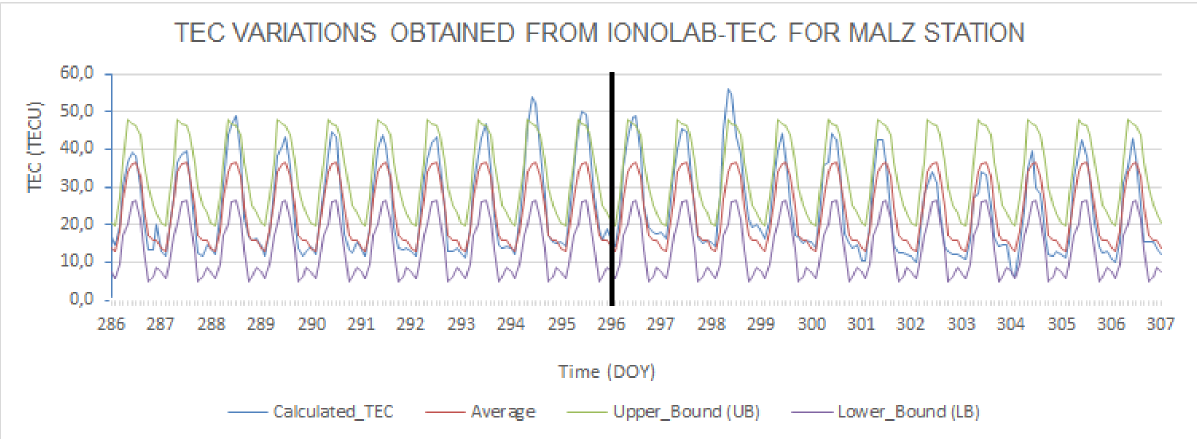

Figure 7. IONOLAB-TEC Values for the MALZ Station

The correlation coefficient ***r*** between the TEC values calculated by both methods for the MALZ station was 0.976587 indicating also a strong positive relationship. The anomaly tables for this station are provided below (Tables 3 and 4).

GIM-TEC Anomaly Table for MALZ Station

Number	DOY	Hour	TEC Difference (TECU)	Type of Anomaly	Number	DOY	Hour	TEC Difference (TECU)	Type of Anomaly
1	288	12	3.5	Positive	5	295	12	3.1	Positive
2	289	12	0.5	Positive	6	296	12	7.9	Positive
3	293	12	3.9	Positive	7	297	12	4.7	Positive
4	294	12	8.6	Positive	8	298	8	12.6	Positive

Table 3. MALZ Station Global Ionosphere Model Anomaly Table

IONOLAB-TEC Anomaly Table for MALZ Station									
Number	DOY	Hour	TEC Difference (TECU)	Type of Anomaly	Number	DOY	Hour	TEC Difference (TECU)	Type of Anomaly
1	288	12	2.3	Positive	5	296	12	2.5	Positive
2	293	12	0.4	Positive	6	298	6	8.6	Positive
3	294	10	7.4	Positive	7	304	0	0.2	Negative
4	295	10	3.6	Positive					

Table 4. MALZ Station IONOLAB-TEC Anomaly Table

Tables 3 and 4 show the anomalies found as a result of the analysis of the TEC values obtained by the IONOLAB-TEC and GIM-TEC methods for the MALZ station. It is believed that the positive anomaly on days 288 and 289 was caused by moderate (136.9 sfu, 150 sfu) solar activity. It is also believed that the anomalies on the days 293, 294, 295 and 296 were caused by strong (157.8 sfu, 166.3 sfu, 162.5 sfu, 153.9 sfu) solar activity.

Below are the TEC values for the OZAL station obtained using the GIM-TEC and IONOLAB-TEC methods for the dates 13 October – 02 November (Figures 10 and 11).

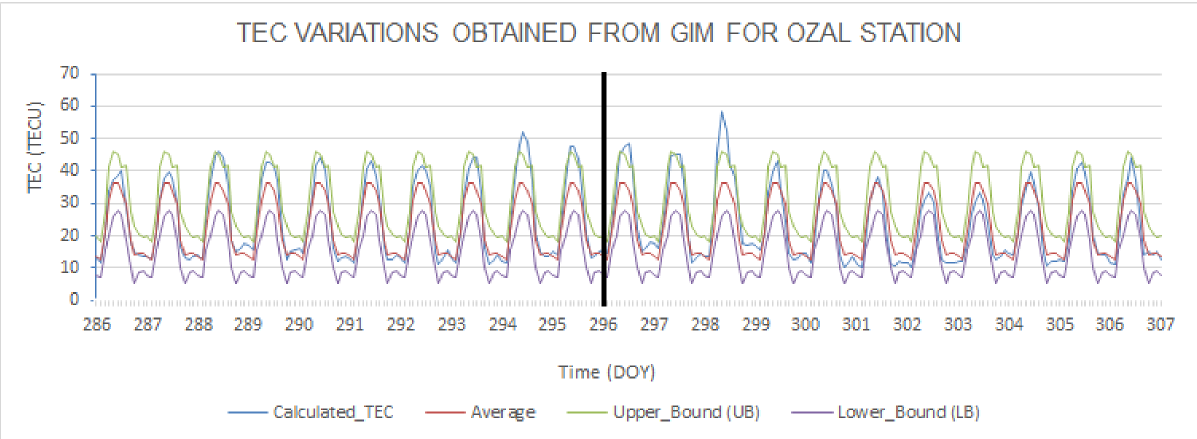

Figure 8. GIM-TEC Values for the OZAL Station

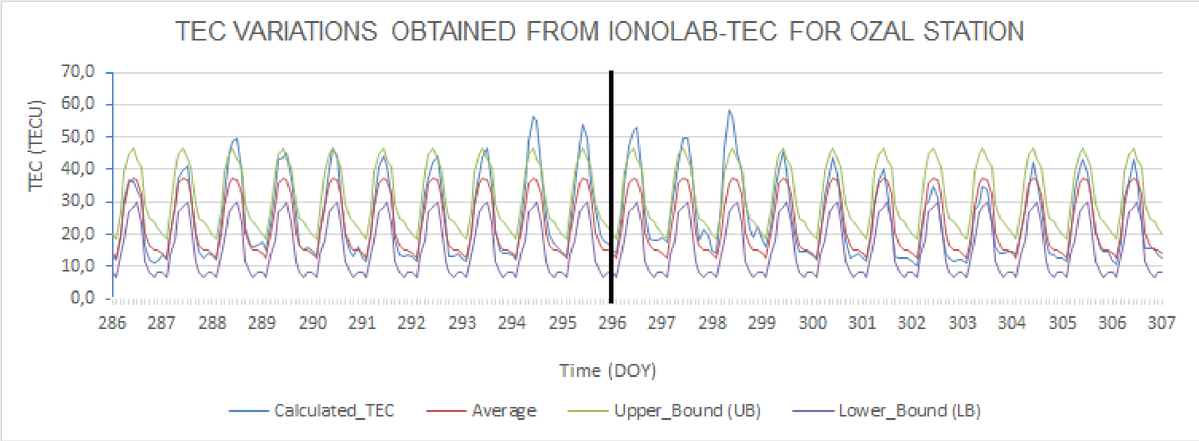

Figure 9. IONOLAB-TEC Values for the OZAL Station

The correlation coefficient *r* between the TEC values calculated by both methods for the OZAL station was 0.982774 demonstrating a strong positive relationship. The anomaly tables for this station are provided below (Tables 5 and 6).

GIM-TEC Anomaly Table for OZAL Station									
Number	DOY	Hour	TEC Difference (TECU)	Type of Anomaly	Number	DOY	Hour	TEC Difference (TECU)	Type of Anomaly
1	288	12	2.8	Positive	5	296	12	7.2	Positive
2	293	12	3.2	Positive	6	297	12	4.0	Positive
3	294	12	7.9	Positive	7	298	8	12.4	Positive
4	295	12	2.4	Positive					

Table 5. OZAL Station Global Ionosphere Model Anomaly Table

IONOLAB-TEC Anomaly Table for OZAL Station									
Number	DOY	Hour	TEC Difference (TECU)	Type of Anomaly	Number	DOY	Hour	TEC Difference (TECU)	Type of Anomaly
1	288	12	6.1	Positive	7	295	10	7.4	Positive
2	289	12	1.6	Positive	8	296	12	9.6	Positive
3	290	12	0.9	Positive	9	297	12	6.0	Positive
4	293	12	3.5	Positive	10	298	8	13.6	Positive
5	292	12	0.6	Positive	11	301	14	1.2	Negative
6	294	12	11.8	Positive	12	302	14	1.4	Negative

Table 6. OZAL Station IONOLAB-TEC Anomaly Table

Below are the TEC values for the TVAN station obtained using the GIM-TEC and IONOLAB-TEC methods (Figures 12, 13).

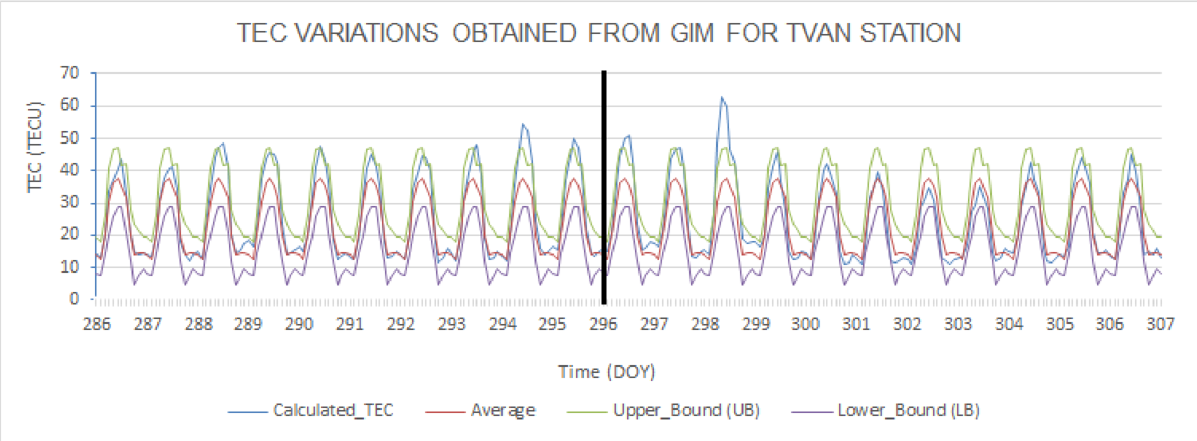

Figure 10. GIM-TEC Values for the TVAN Station

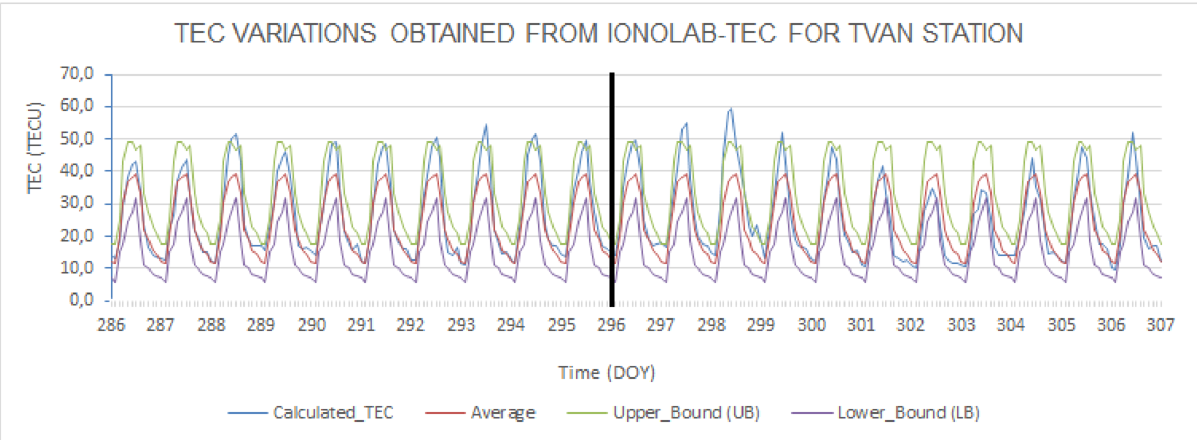

Figure 11. IONOLAB-TEC Values for the TVAN Station

The correlation coefficient between the TEC values calculated by both methods for the TVAN station was 0.978363 representing a strong positive relationship. The anomaly tables for this station are provided below (Tables 7 and 8).

GIM-TEC Anomaly Table for TVAN Station

Number	DOY	Hour	TEC Difference (TECU)	Type of Anomaly
1	286	12	2.1	Positive
2	288	12	7.0	Positive
3	289	12	3.5	Positive
4	290	12	1.8	Positive
5	292	12	2.8	Positive
6	293	12	6.4	Positive
10	294	12	11.0	Positive
11	295	12	5.4	Positive
12	296	12	9.3	Positive
13	297	12	5.5	Positive
14	298	8	16.5	Negative

Table 7. TVAN Station Global Ionosphere Model Anomaly Table

IONOLAB-TEC Anomaly Table for TVAN Station									
Number	**DOY**	**Hour**	**TEC Difference (TECU)**	**Type of Anomaly**	**Number**	**DOY**	**Hour**	**TEC Difference (TECU)**	**Type of Anomaly**
1	288	12	5.1	Positive	10	296	12	3.4	Positive
2	290	12	2.6	Positive	11	297	12	8.5	Positive
3	291	12	2.0	Positive	12	298	10	10.5	Positive
4	292	12	4.0	Positive	13	299	10	2.8	Positive
5	293	12	8.1	Positive	14	302	12	0.7	Negative
6	294	12	5.1	Positive	15	306	10	2.9	Positive
7	295	12	3.2	Positive					

Table 8. TVAN Station IONOLAB-TEC Anomaly Table

Tables 1, 2, 3, 4, 5, 6, 7 and 8 show the results of the statistical analysis of the TEC values created by the IONOLAB-TEC and GIM-TEC methods. The tables also depict the day and hour in which anomalies were observed, and the quantity and type of the anomaly. The numbers of anomalies obtained in both models were very close to each other. The F10.7 cm index values between the days 286 and 292 were 136 sfu, 135.4 sfu, 136.9 sfu, 150 sfu, 151.6 sfu, 145.7 sfu, 146.1 sfu. The index values show that there was usually moderate solar activity. Therefore, the anomalies in question may be related to the earthquake or solar activity. The index values for the days 293, 294, 295 and 296 (the day of the earthquake) were 157.8 sfu, 166.3 sfu, 162.5 sfu and 153.9 sfu respectively. These values indicate strong solar activity. On the other hand, the ionosphere layer was calm in these days in terms of geomagnetic conditions. As there was strong solar activity, the numbers of anomalies were higher than the numbers in the days 286-292. Since solar activity was moderate in the day 297, the number of anomalies dropped. The solar activity on the day 298 was moderate, but there was strong geomagnetic activity (Dst -147 nt, Kp*10=73). The reason for the high numbers of anomalies on day 298 in both models is believed to be due to geomagnetic activity. Considering the analyzed days in general, it may be seen that it is difficult to identify earthquake-related anomalies as the solar activity and geomagnetic conditions before and after the earthquake were not calm. Therefore, it is believed that the anomalies detected in the stations on days 293-296 may be related to the earthquake and/or solar activity, and the anomalies on days 297 and 298 may be related to the earthquake, solar activity and/or geomagnetic activity.

4. CONCLUSION

In the scope of this study, the TEC values for the stations HAKK, MALZ, OZAL, TVAN were obtained using the GIM-TEC and IONOLAB-TEC methods. In the comparison of the obtained values, it was seen that there was high correlation between the TEC values obtained by the two models. In order to detect earthquake-related TEC changes better, the TEC values created from both models for the period of 13.10.2011-02.11.2011 were used as reference to determine the UB and LB values. As a result of the statistical test, anomalies were found in all analyzed stations for before, on the day of and after the earthquake. In order to understand whether the anomalies obtained in both models were earthquake-related, the ionospheric conditions, geomagnetic activity and solar activity on the analyzed days were examined using the Kp, Dst and F10.7 cm indices.

Consequently, it was determined that the positive anomalies observed on days 286-292 may be related to moderate solar activity and/or the earthquake, and the positive anomalies observed on days 293, 294, 295, 296 (day of the earthquake) may be related to strong solar activity and/or the earthquake. Moderate solar activity and strong geomagnetic activity were observed for day 298, so the numbers of anomalies in both models increased dramatically. This increase is considered to be related to geomagnetic activity. The anomaly on day 298 may be related to the earthquake, geomagnetic effects and/or solar activity. The finding that the ionospheric conditions were vibrant in the analyzed days makes it highly difficult to identify earthquake-related ionospheric changes. Therefore, interdisciplinary studies are needed to determine the earthquake-related part of the change in question.

REFERENCES:

Akhoondzadeh, M., De Santis, A., Marchetti, D., Piscini, A., & Cianchini, G. (2018). Multi precursors analysis associated with the powerful Ecuador (MW= 7.8) earthquake of 16 April 2016 using Swarm satellites data in conjunction with other multi-platform satellite and ground data. *Advances in Space Research*, *61*(1), 248-263.

Anderson, D., & Fuller-Rowell, T. (1999). The ionosphere. Boulder, CO (325 Broadway, Boulder 80303-3326): Space Environment Center

Arikan F, Erol C B and Arikan O (2003) Regularized Estimation Of Vertical Total Electron Content From Global Positioning System Data, Journal of Geophysical Research. 118, 1469-1480, 2003

Arikan F, Erol C B and Arikan O (2004) Regularized Estimation of Vertical Total Electron Content from GPS Data for a Desired Time Period, Radio Science, 39:RS6012,**.**

Arikan F, Arikan O and Erol C B (2007) Regularized estimation of TEC from GPS data for certain midlatitude stations ve comparison with IRI model Cospar, Advances In Space Research, ISSN: 0273-1177, Vol.39.

Aslan N (2004) GPS ile İyonosfer Toplam Elektron Yoğunluğu Değişimlerinin Koordinatlara Etkisinin Araştırılması Doktora Tezi, Yıldız Teknik Üniversitesi, Fen Bilimleri Enstitüsü.

Aysezen M S (2008) Türkiye için IONOLAB-TEC Kullanılarak GPS Tabanlı TEM ve Alıcı Yanlılığı Veri Tabanı Hazırlanması, Yüksek Lisans Tezi, Zonguldak Karaelmas Üniversitesi.

Başpınar S (2012) CORS-TR Verileriyle İyonosfer Modellerinin İncelenmesi, Doktora Tezi, İstanbul Ticaret Üniversitesi, Fen Bilimleri Enstitüsü**.**

Barnes R A andLeonard R S (1965) Observations of ionospheric disturbances following the Alaska earthquake. J GeophysRes70: 1 250−1 253.

Erol C.B., Arıkan F., (2004), "GPS Sinyalleri ile İyonosferin İstatistiksel Özelliklerinin Belirlenmesi"., URSI-Türkiye., İkinci Ulusal Kongresi, 2004.

Erol C.B., Arıkan F., (2005), "Statistical Chracterization of the Ionosphere Using GPS Signals"., J. of Electromagnetic Waves an Appl., Vol.19, No:3, 2005.

Gümrükçü O (2009) GPS Sinyalleri İle Konum Belirlemede İyonosferik Etkilerin İncelenmesi Yüksek Lisans Tezi, Yıldız Teknik Üniversitesi, Fen Bilimleri Enstitüsü.

He, L., & Heki, K. (2017). Ionospheric anomalies immediately before Mw 7.0-8.0 earthquakes. *Journal of Geophysical Research: Space Physics*.

He, L., Wu, L., Pulinets, S., Liu, S., & Yang, F. (2012). A nonlinear background removal method for seismo-ionospheric anomaly analysis under a complex solar activity scenario: A case study of the M9. 0 Tohoku earthquake. *Advances in Space Research*, *50*(2), 211-220.

İnyurt S (2015) İyonosferdeki Toplam Elektron Miktarı (Tec) Ve Kod Yanlılık Değerlerinin (DCB) GNSS Ölçümleriyle Belirlenmesi Yüksek Lisans Tezi, Bülent Ecevit Üniversitesi, Fen Bilimleri Enstitüsü.

Kelley, M. C., Swartz, W. E., & Heki, K. (2017). Apparent ionospheric total electron content variations prior to major earthquakes due to electric fields created by tectonic stresses. *Journal of Geophysical Research: Space Physics*.

Langley R B (2002) Monitoring the Ionosphere and Neutral Atmosphere with GPS Division of Atmospheric and Space Physics Workshop, Frederiction, N.B., 21-23 February 2002.

Li, M., & Parrot, M. (2017). Statistical analysis of the ionospheric ion density recorded by DEMETER in the epicenter areas of earthquakes as well as in their magnetically conjugate point areas. *Advances in Space Research*.

Liu, J. Y., Chen, C. H., Chen, Y. I., Yang, W. H., Oyama, K. I., & Kuo, K. W. (2010). A statistical study of ionospheric earthquake precursors monitored by using equatorial ionization anomaly of GPS TEC in Taiwan during 2001–2007. *Journal of Asian Earth Sciences*, *39*(1-2), 76-80.

Mekik Ç (1999) GPS' e Atmosferin Etkileri, TMMOB Harita ve Kadastro Mühendisleri Odası Dergisi, Sayı: 86.

Pulinets S. A. (1998), "Strong earthquakes prediction possibility with the help of top side sounding from satellites". Advances in Space Research 21(3): 455−458.

Pulinets, S., & Davidenko, D. (2014). Ionospheric precursors of earthquakes and global electric circuit. *Advances in Space Research*, *53*(5), 709-723.

Rozhnoi, A., Solovieva, M., Parrot, M., Hayakawa, M., Biagi, P. F., Schwingenschuh, K., & Fedun, V. (2015). VLF/LF signal studies of the ionospheric response to strong seismic activity in the Far Eastern region combining the DEMETER and ground-based observations. *Physics and Chemistry of the Earth, Parts A/B/C*, *85*, 141-149.

Schaer S (1999) Mapping and Predicting the Earth's Ionosphere Using the Global Positioning System, Doktora Tezi, University of Bern, İsviçre.

Schaer, S., W. Gurtner, and J. Feltens, IONEX: The IONosphere Map EXchange format Version 1, in Proceedings of the IGS Analysis Center Workshop, edited by J. M. Dow, J. Kouba, and T. Springer, Darmstadt, February 9 – 11, 1998.

Ünver O (2010) İyonosferik Toplam Elektron İçeriği (TEC) Değişiminin Belirlenmesi Yüksek Lisans Tezi, Yıldız Teknik Üniversitesi, Fen Bilimleri Enstitüsü.

Yildirim, O., Inyurt, S., Mekik, C. (2016). Review of variations in Mw< 7 earthquake motions on position and TEC (Mw= 6.5 Aegean Sea earthquake sample). *Natural Hazards and Earth System Sciences*, *16*(2), 543-557.

URL-1 www.ionolab.org.tr

URL-2 https://omniweb.gsfc.nasa.gov/form/dx1.html